

Interpretation of the Wingless Gradient Requires Signaling-Induced Self-Inhibition

Eugenia Piddini¹ and Jean-Paul Vincent^{1,*}

¹MRC National Institute for Medical Research, Mill Hill, London NW7 1AA, UK

*Correspondence: jvincen@nimr.mrc.ac.uk

DOI 10.1016/j.cell.2008.11.036

SUMMARY

In a classical view of development, a cell can acquire positional information by reading the local concentration of a morphogen independently of its neighbors. Accordingly, in *Drosophila*, the morphogen Wingless produced in the wing's prospective distal region activates target genes in a dose-dependent fashion to organize the proximodistal pattern. Here, we show that, in parallel, Wingless triggers two nonautonomous inhibitory programs that play an important role in the establishment of positional information. Cells flanking the source of Wingless produce a negative signal (encoded by *notum*) that inhibits Wingless signaling in nearby cells. Additionally, in response to Wingless, all prospective wing cells produce an unidentified signal that dampens target gene expression in surrounding cells. Thus, cells influence each other's response to Wingless through at least two modes of lateral inhibition. Without lateral inhibition, some cells acquire ectopic fates. Lateral inhibition may be a general mechanism behind the interpretation of morphogen gradients.

INTRODUCTION

The morphogen concept provides a fundamental framework to understand pattern formation in multicellular organisms (Turing, 1952; Wolpert, 1969; Lawrence, 2001). In simple terms, cells within a field acquire positional information by "reading" the local concentration of a diffusible signal, which is typically produced from a localized source. Several developmental signals, including members of the TGF β , Hedgehog, and Wnt families, have been identified as morphogens, and this has triggered numerous studies aimed at understanding how the distribution of morphogens is regulated and how morphogen gradients are interpreted. Overall, the results support the traditional view that the graded distribution of a ligand could specify distinct cell fates (Ashe and Briscoe, 2006; Fuccillo et al., 2006). However, this view raises fundamental issues about robustness of the gradient and about the ability of cells to measure different morphogen levels.

The regulatory mechanisms that contribute to the formation of robust gradients have been extensively discussed (Eldar et al., 2003, 2004; Jaeger et al., 2008). Here, we consider the issue of gradient interpretation. So far, it has generally been assumed that cells are independent agents endowed with a capacity to read the local morphogen concentration (Gurdon et al., 1998, 1999; Gurdon and Bourillot, 2001) and to translate it into appropriate cell fates. Cells use sophisticated strategies in order to express the right target genes at a given morphogen level (Ashe and Briscoe, 2006; Dessaud et al., 2007). However, recent theoretical studies have questioned whether a single morphogen profile has sufficient information content to specify different, closely spaced cell fates in a reliable manner (Howard and ten Wolde, 2005; McHale et al., 2006). For example, physical considerations suggest that individual nuclei alone cannot accurately "measure" the observed concentrations of the Bicoid morphogen within early *Drosophila* embryos (Gregor et al., 2007). One way for an organism to increase positional information content within a field is to deploy two opposing gradients instead of one. For example, in the chick neural tube, cell fate specification relies on Sonic Hedgehog (Shh) derived from the floor plate on the ventral side, as well as on Bone Morphogenetic Protein (BMP) originating from the dorsal side (Liem et al., 2000; Patten and Placzek, 2002). However, when a single gradient is present, as in the case of Bicoid at the anterior of early *Drosophila* embryos, some form of secondary processing (such as spatial averaging among neighboring nuclei) could help improve gradient readout (Gregor et al., 2007). This view is echoed in a recent review, which argues that, without additional cell interactions, a single morphogen may provide only crude positional information (Kerszberg and Wolpert, 2007). Therefore, secondary processing of morphogen gradients has been predicted, but no experimental example has been reported. It is therefore timely to reinvestigate experimentally how known morphogens gradients are interpreted.

Members of the Wnt family of secreted glycolipoproteins have been suggested to act as morphogens during rostrocaudal patterning of the vertebrate neural tube (Kiecker and Niehrs, 2001; Nordstrom et al., 2002). Likewise, extensive evidence suggests that Wingless (Wg), a *Drosophila* member of the Wnt family, acts as a morphogen, especially in wing imaginal discs (Zecca et al., 1996; Strigini and Cohen, 1999; Vincent and Briscoe, 2001). In this tissue, during the third larval instar, Wg is expressed in a stripe of cells straddling the dorsoventral (D/V) boundary.

From there, Wg spreads symmetrically to activate genes in at least three nested domains within the prospective wing, an area of the disc called the pouch. Close to the Wg source, so called high-level target genes such as *senseless* (*sens*), *achaete*, and *neuralized* are expressed. In a more extended range (up to ~20 cell diameters), the *distalless* (*dll*) gene is expressed. Finally, *vestigial* (*vg*), a low-level target gene, is expressed in most of the prospective wing. Importantly, expression of these target genes requires direct action of Wg since it is greatly reduced in clones of cells that are unable to transduce the signal (Chen and Struhl, 1999; Neumann and Cohen, 1997; Zecca et al., 1996). Moreover, gain-of-function experiments have shown that ectopic activation of the Wg pathway in the pouch triggers target gene expression in a manner that indicates dose-dependent action (Neumann and Cohen, 1997; Zecca et al., 1996). Although the view that Wg acts as a morphogen in the wing pouch is widely accepted, an alternative has been suggested, namely that Wg may be required merely to reinforce a pre-existing pattern of gene expression (Klein and Arias, 1999; Martinez Arias, 2003). Consistent with this view, the prior presence of Vg is required for Wg to positively modulate Vg expression (Zecca and Struhl, 2007).

In this paper, we investigate how the Wg gradient is interpreted in *Drosophila* imaginal discs. We show that two additional regulatory mechanisms, initiated by Wg and superimposed on the Wg gradient, contribute to proximodistal patterning of the wing. First, in response to high-level Wg signaling, cells in the distal region produce a secondary negative signal (encoded by *notum*) that laterally inhibits Wg target genes in neighboring cells. Second, in response to the Wg signal, all prospective wing cells produce a negative signal that represses target genes in their surrounding area (another form of secondary lateral inhibition). We suggest that these two modes of negative regulation enable cells to precisely and reliably compute their positional value within the Wg gradient.

RESULTS

Maintenance of *dll* and *vg* Expression after Removal of Wingless Signaling

To investigate the role of Wg during imaginal disc development, we generated homozygous *wg* mutant cells by Flp-mediated mitotic recombination (Xu and Rubin, 1993). A *Ubx-Flp* transgene was used to induce widespread recombination in the prospective wing area. Furthermore, homozygous mutant cells were given a growth advantage with the *Minute* technique (Morata and Ripoll, 1975). Thus, with the *Ubx-Flp Minute* system, imaginal discs become progressively depleted of *wg*-expressing cells during the second and third larval instars (Figures 1D and 1D', compare to wild-type in Figure 1C) and are mostly devoid of Wg at the end of the third larval instar (Figures 1B and 1B', compare to wild-type in Figure 1A). These discs look almost normal and give rise to relatively well-patterned wings in eclosing adults. Apart from two recognizable defects, the loss of margin bristles (which require high-level Wg signaling for their specification; Phillips and Whittle [1993]) and a reduction of wing size, the overall wing shape and the vein pattern are near-normal (Figures 1E and 1F). This is a surprising result considering the key role attributed to Wg in wing patterning.

We next looked at the expression of previously identified Wg target genes in wing discs lacking *wg*-expressing cells. As expected from the adult wing phenotype, *sens*, which is normally activated at the mid-third instar to specify margin bristles (Nolo et al., 2000), fails to be expressed (data not shown, but see Figure 2D'). Surprisingly however, the mid- and low-level target genes *dll* and *vg*, whose expression is initiated at the first/second instar, are largely unaffected in the absence of Wg. The profiles of both *dll* (Figures 1G–1J) and *vg* (data not shown) are slightly narrower than those of control discs, but peak intensities levels are normal. To exclude the possibility that another Wnt might compensate for the loss of Wg in *wg* mutant discs, we used the *Ubx-Flp Minute* system to generate discs lacking the Wg receptors Frizzled (*Fz*) and Frizzled2 (*Fz2*). Lack of both receptors causes loss of Wg signaling (Chen and Struhl, 1999). Like *wg* mutant discs, *fz fz2*-deficient discs express *dll* and *vg* at apparently normal levels, albeit over a slightly reduced range (Figure S1 available online and data not shown). Therefore, despite an early requirement for Wg signaling in wing specification during the first and second larval instars (Morata and Lawrence, 1977; Ng et al., 1996; Sharma and Chopra, 1976; Wang et al., 2000; Wu and Cohen, 2002), sustained Wg signaling is not required for continued expression of *dll* and *vg*.

As we have shown, expression of *dll* and *vg* is relatively unaffected in third larval instar discs that completely lack Wg signaling, yet expression of these genes is not maintained in small clones of cells that cannot transduce the Wg signal. For example, *fz fz2* mutant clones induced by a heat-inducible Flp transgene (*hs-Flp*) lose *dll* expression in a cell-autonomous manner, even if these clones are generated during the third larval instar (Chen and Struhl, 1999; Jaiswal et al., 2006). To confirm this result, small *fz fz2* mutant clones were induced with *Ubx-Flp* (i.e., at the same developmental stage as above) but in a *Minute^{+/+}* background so that mutant cells do not gain a growth advantage. Under such conditions, mutant tissue (marked by the absence of GFP) continues to coexist with wild-type tissue, even up to the late third-instar stage (Figure 1K). In these discs, both *dll* (Figure 1K') and *vg* (data not shown) are downregulated within the mutant tissue, consistent with previous reports. We conclude that loss of Wg signaling has different effects on the expression of these two target genes depending on whether the loss occurs in small patches of tissue or in the whole disc.

To directly compare target gene expression in groups of Wg-deficient cells with that in control wild-type tissue, we made the entire posterior (P) compartment mutant, leaving the anterior (A) compartment unaffected. Mutant clones were induced by expressing a *UAS-Flp* transgene throughout the P compartment (with *engrailed-Gal4* [*en-Gal4*] or *hedgehog-Gal4* [*hh-Gal4*]). As before, mutant cells were given a growth advantage by the introduction of a *Minute* mutation in the background. This combination causes the P compartment of resultant imaginal discs to become entirely homozygous mutant while the A compartment remains wild-type. Although such P compartments are reduced in size, they express *dll* relatively normally (Figures 2A and 2A'). Fluorescence intensity quantification (Figures 2B and 2B') reveals that, except for a subtle reduction of *dll* expression in P cells located near the D/V boundary (where Wg would normally be expressed), the *dll* expression profiles are similar in the two

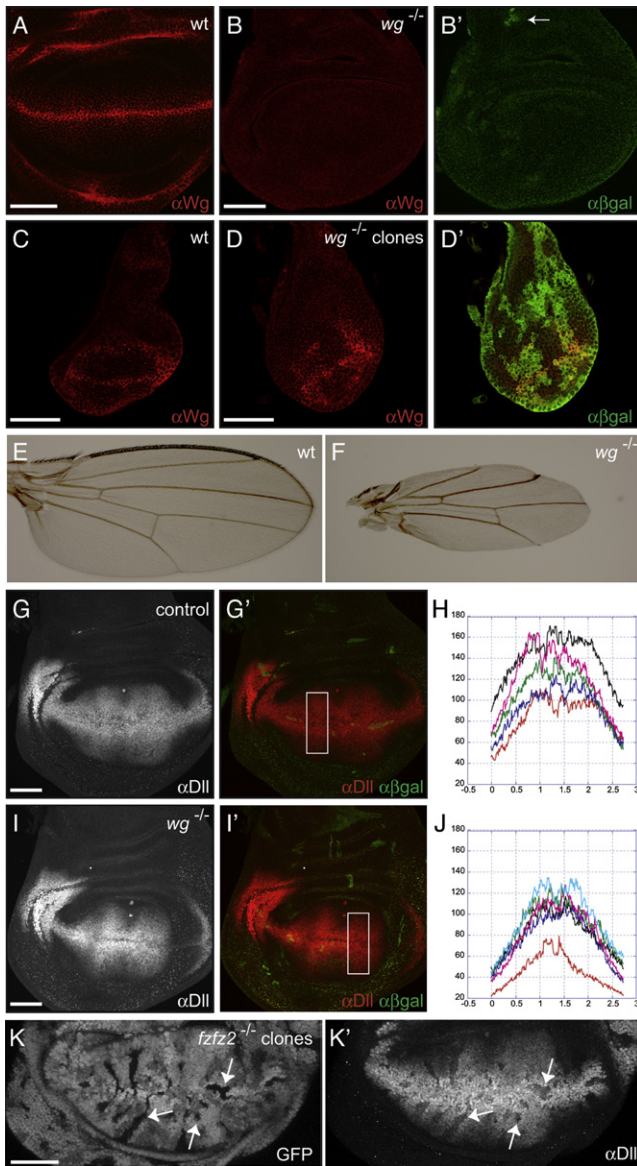


Figure 1. Expression of *dll* in the Absence of Wg

(A) Wild-type, late third instar wing imaginal disc stained with anti-Wg. (B and B') Imaginal disc from a late third instar larva of genotype *Ubx-FLP; wg FRT/ M(2) FRT*. Anti-Wg staining shows that no Wg-expressing cell remains (B). The absence of β-galactosidase, which marks *wg*^{-/-} cells, confirms that the disc is almost entirely made of mutant cells (B'). Arrow in (B') points to small patch of residual β-galactosidase-positive heterozygous tissue. (C) Wg protein in a wild-type wing imaginal disc from an early third instar larva. (D and D') Imaginal disc from an early third instar larva of same genotype as in (B) and (B') double-stained with anti-Wg (D) and anti-β-galactosidase (D'). At this stage, several heterozygous (β-galactosidase-positive) patches remain, hence the presence of Wg immunoreactivity. (E) Wing from a wild-type fly. (F) Wing from a fly of the same genotype as in (B) (i.e., no Wg at mid-late third instar). (G and G') Imaginal disc from control late third instar larvae stained as indicated. Genotype is *Ubx-FLP; FRT/ M(2) FRT*. Wg expression is normal (data not shown). (H) Horizontally averaged fluorescent intensity profiles of anti-DII staining in control discs. An area (as that boxed in [G']) was selected in five different discs, and one profile is displayed for each disc.

compartments, both in terms of range and intensity. Similarly, *vg* appears to be expressed relatively normally in P compartments lacking Wg (Figures 2C and 2C'). In contrast, expression of *sens*, which is considered a high-level target gene, is consistently lost in Wg-deficient tissue (Figures 2D and 2D'). This is not specific to high-level target genes, however, because *fz3*, a Wg target gene normally broadly expressed on either side of the Wg source (Sato et al., 1999; Sivasankaran et al., 2000), is also lost (data not shown). Because no Wg protein can be detected in the P compartment of these discs (except in P cells located within two to three cell diameters of the A compartment, Figures 2A and 2C), it seems unlikely that Wg produced in the A compartment could spread throughout the P compartment to rescue *dll* or *vg* expression there. Nevertheless, to rule out the possibility of nonautonomous rescue, we generated discs with P compartments lacking *fz fz2* and assessed target gene expression. About two-thirds of these discs had severely underdeveloped or absent P compartments. This is probably because early loss of Wg signaling interferes with wing specification, as the *en-Gal4 UAS-Flp* system generates clones in the embryo, even before the first instar. However, and importantly, about one-third of the discs in this experiment developed relatively normally up to the third instar, presumably because, by chance, a sufficient number of P cells were able to acquire the wing disc fate. In such discs, no reduction of *dll* expression (Figures 2E and 2E') and only a mild reduction in *vg* expression (data not shown) are seen in the P compartment. *Sens* was consistently absent from *fz fz2*-deficient P compartments (data not shown).

As before with *Ubx-Flp*, we performed a control experiment whereby *fz fz2* mutant cells were induced in the P compartment with *en-Gal4 UAS-Flp* but without being given a growth advantage. These clones remained interspersed with wild-type tissue throughout development and downregulated all three target genes tested, as expected (*dll*, Figures 2F and 2F'; *vg* and *sens*, data not shown). We conclude that removal of Wg signaling in cells that are surrounded by wild-type cells causes the loss of *dll* and *vg* expression, whereas removal in the whole P compartment has only a minor effect on expression of these genes. To exclude the possibility that the above results might be an artifact of the Minute technique, we used three alternative means of achieving compartment-wide removal of Wg. The results, illustrated in Figures S2 and S3 and described in the accompanying

(I and I') Imaginal disc from a late third instar larva of genotype *Ubx-FLP; wg FRT/ M(2) FRT* (no *wg*-expressing cell left). Staining is as in (G) and (G'). The lack of β-galactosidase shows that most cells are homozygous *wg* mutant. Expression of *dll* appears normal (compare to control discs in [G] and [G']). (J) Anti-DII fluorescence intensity profiles from six discs show that a relatively normal DII gradient forms despite the absence of Wg.

(K and K') Wing disc from a *Ubx-FLP; fz fz2* mutant larva stained with GFP (E) and anti-DII (E). Here, *fz fz2* mutant (GFP-negative) clones are interspersed among wild-type (GFP-positive) cells. Note the downregulation of *dll* expression in *fz fz2* mutant clones (arrows). In this and all subsequent figures, discs are taken from late third instar larvae.

See the **Experimental Procedures** for detailed genotypes used in this and all subsequent figures. In all figures, the absence of GFP (or β-galactosidase) marks mutant territories. GFP- (or β-galactosidase-) expressing cells retain at least one wild-type allele and hence will be referred to as "wild-type." Throughout, scale bars are 50 μm, anterior is to the left, and dorsal is on top.

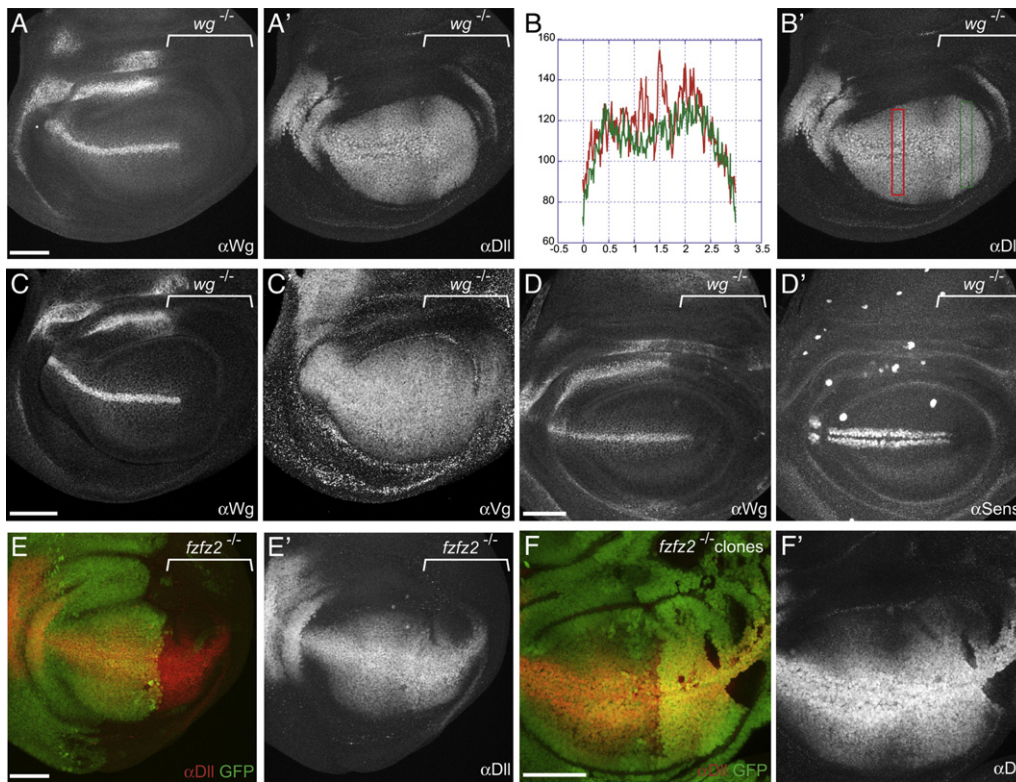


Figure 2. Expression of *dll*, *vg*, and *sens* in Posterior Compartments Lacking Wg Signaling

(A–D') Wing discs of genotype *FRT wg / FRT M(2); hh-Gal4 UAS-FLP* (no Wg produced in P compartment) stained as indicated. Expression of *dll* is relatively unaffected by the absence of Wg in the P compartment (A'). This is confirmed by the anti-Dll intensity profiles shown in (B). The green profile corresponds to the green box in the posterior (*wg* mutant) compartment and the red profile corresponds to the red box in the control anterior compartment (shown in [B']). The range and intensities of *dll* expression are similar in the two compartments, except for a relative reduction in intensity near the D/V boundary in the mutant compartment (where Wg would have been produced). Expression of *vg* is also largely unaffected by the absence of Wg in the P compartment (C and C'). By contrast, *sens* expression is lost in *wg* mutant P compartments (D and D').

(E and E') Wing discs of the genotype *en-Gal4 UAS-FLP; fz fz2 FRT / M(3) FRT* (no Wg signal transduction in the P compartment) stained with anti-Dll ([E], red, and [E'], white). GFP is shown in green. Dll is expressed in an apparently normal fashion ([E']), compare Dll staining in mutant, GFP-negative, P cells with that in control A cells. (F and F') Wing discs of the genotype *en-Gal4 UAS-FLP; fz fz2 FRT / FRT* stained with anti-Dll ([F], red, and [F'], white). GFP is shown in green. Here, *fz fz2* mutant cells (GFP-negative) remain in clones surrounded by wild-type tissue. Note the marked downregulation of *dll* in the mutant tissue.

legends, confirm our conclusion that Wg signaling is not required for continued expression of *dll* and *vg* during the third instar, the major period of disc growth.

axin Mutant Cells Suppress All Target Gene Expression in Nearby Wild-Type Cells

Our results show that, in mosaic imaginal discs, the presence of wild-type cells renders Wg receptor-deficient cells incapable of *dll* and *vg* gene expression. One possibility is that receipt of the Wg signal makes cells produce a secondary negative signal that itself suppresses target gene expression in receptor-deficient cells. We therefore asked whether overactivation of Wg signaling in clones causes downregulation of target genes in remaining wild-type cells. To overactivate signaling in demarcated groups of cells, we used a mutation in *axin*. *axin* mutant cells cannot degrade Armadillo/ β -Catenin and therefore hyperactivate the Wg pathway in a ligand-independent fashion (Hart et al., 1998; Ikeda et al., 1998; Zeng et al., 1997).

As expected, small *axin* mutant clones generated by *hs-Flp*-induced recombination strongly upregulate the expression of *dll* (Figures 3A and 3A') (see also Hamada et al., 1999) and *vg* (data not shown). In addition, in several instances, *dll* expression is depressed in wild-type cells immediately juxtaposed to *axin* mutant clones. This is best illustrated by fluorescence intensity measurements, as shown in Figures 3B and 3B'. It appears therefore that high-signaling cells inhibit target gene expression in nearby wild-type cells. To further investigate this nonautonomous suppressive effect, we generated large *axin* clones. If *axin* mutant cells are given a growth advantage with the *Minute* technique, most of the disc becomes mutant and only small patches of wild-type cells remain. Strikingly, even though they are capable of transducing the Wg signal, these residual wild-type cells downregulate *dll* (Figures 3C and 3C' and inset in same figure) and *vg* (data not shown). This reduction in target gene expression is not due to loss of Wg expression since Wg is expressed normally in discs harboring large *axin* clones (as seen by anti-Wg staining; data not shown).

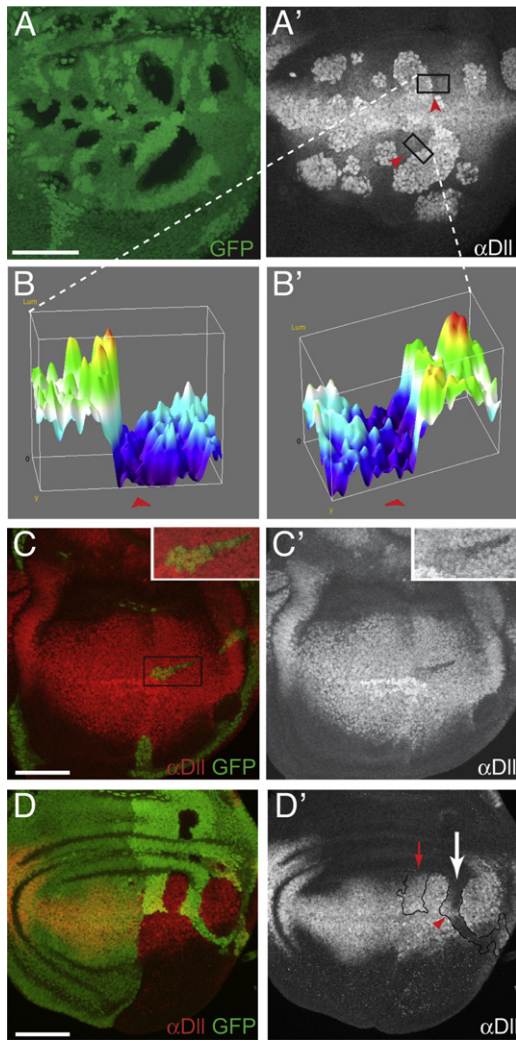


Figure 3. *axin* Mutant Cells cause *dll* Downregulation in Neighboring Wild-Type Cells

(A and A') Wing discs with small *hs-FLP*-induced *axin* clones stained with anti-Dll (A'). Lack of GFP ([A], green) marks the clones. All the mutant clones show a marked increase in Dll expression. Note the repression of *dll* expression in wild-type (GFP-positive) cells surrounding the clones. Boxed areas indicate the ROIs used to generate intensity plots.

(B and B') 3D fluorescence intensity surface plots from ROIs outlined in (A') (highest intensity is shown in red and lowest in purple). (B) represents the top rectangle in (A'), and a red arrowhead marks equivalent positions in (A') and (B). Likewise, the red arrowhead included in (B') represents the bottom rectangle in (A'). As expected, high fluorescence intensity is seen inside the *axin* mutant clones. Note that the intensity is lower in wild-type cells abutting the clones than in those further away.

(C and C') Wing disc from a *hs-FLP*; *FRT axn/M(3) FRT* larva stained with anti-Dll (red in [C], white in [C']). As a result of the "Minute" growth advantage, *axin* mutant cells (GFP-negative in [C]) colonize most of the disc, leaving only small patches of wild-type (GFP-positive) cells that downregulate *dll* expression (shown in the inset).

(D and D') Wing disc from *en-Gal4 UAS-FLP*; *FRT axn/FRT* larvae stained as indicated. In these discs, the A compartment is wild-type and provides an internal measure of normal *dll* expression. The P compartment is a mosaic of *axin* mutant (GFP-negative) and wild-type (GFP-positive) cells. Note the downregulation of *dll* in a long patch of posterior wild-type cells (white arrow

In a separate set of experiments, *en-Gal4 UAS-Flp* was used to generate mosaic P compartments containing wild-type (GFP-positive) and *axin* mutant (GFP-negative) cells. In these discs, no clones are formed in the A compartment, which can therefore be used as a reference for the normal level of *dll* expression (Figure 3D). We find that the presence of *axin* mutant cells leads to suppression of *dll* expression in 50% ($n = 24$) of the remaining patches of wild-type cells that do not contact the A/P boundary (Figure 3D', white arrow). Remarkably, wild-type cells that abut the A/P boundary ($n = 19$) seem unaffected by the presence of large *axin* mutant clones (Figures 3D and 3D', red arrow), perhaps because the A/P boundary produces a signal that activates *dll*, thus overriding the negative effect of *axin* clones. One likely such signal is Dpp. Indeed, *tkv* mutant cells, which are unable to transduce the Dpp signal, often downregulate *dll* expression (Figure S4). We conclude that increased Wg signal transduction within *axin* mutant cells can cause the downregulation of *dll* expression in wild-type cells, except in those that are near the anterior-posterior boundary. To ask whether nonautonomous suppression of target gene expression is a general consequence of high Wg signaling, we assessed the effect of adenomatous polyposis coli (APC)-deficient cells, which also strongly overactivate Wg signaling (Akong et al., 2002). Like *axin* mutant cells, they caused the suppression of *dll* expression in residual wild-type cells (Figure S5).

One additional feature of *axin* mutant patches is consistent with the existence of a negative signal downstream of Wg signaling. As noted above, *dll* expression is upregulated in small *axin* patches (Figures 3A and 3A') (Hamada et al., 1999). However, this is not the case when they occupy the majority of a compartment. Fifty-two percent ($n = 31$) of *axin* clones induced by *en-Gal4 UAS-Flp* showed no significant increase in *dll* expression, with the A compartment used as a reference. This is illustrated in Figure 3D', where it can be seen that *dll* expression in mutant (GFP-negative) tissue is comparable to that at the equivalent position in the control A compartment. This observation suggests that *axin* mutant cells suppress each other's ability to upregulate target gene expression and that mutual suppression overrides intrinsic activation when the patches of *axin* mutant tissue are sufficiently large. Interestingly, the decision of *axin* cells to upregulate (or not) target gene expression, a form of normalization, appears to be coherent within a clone.

So far, we have only characterized the effect of *axin* mutant cells on the expression of *dll* and *vg*, two target genes that do not require continuous Wg signaling. Do *axin* mutant cells also suppress the expression of *sens* and *fz3*, two genes that continuously require Wg signaling? Expression of both *fz3* and *sens* is largely suppressed in wild-type cells located near large patches of *axin* mutant cells (Figures 4A and 4B). Unlike

in [D']). Within this patch, residual *dll* expression is seen in the cells that are located near the D/V boundary (red arrowhead) probably because cells are exposed to high level of Wg in this area. Downregulation of *dll* is seen in 50% of wild-type patches that do not contact the A/P boundary ($n = 24$). Downregulation is not seen in patches that contact the A/P boundary (red arrow in [D']; $n = 19$). Note also in (D') that *axin* mutant cells fail to upregulate *dll* (compare mutant tissue in P compartment to wild-type tissue in A compartment). This is true in 52% of *axin* patches analyzed from this genotype ($n = 31$). The black outline in (D') marks the mosaic boundary.

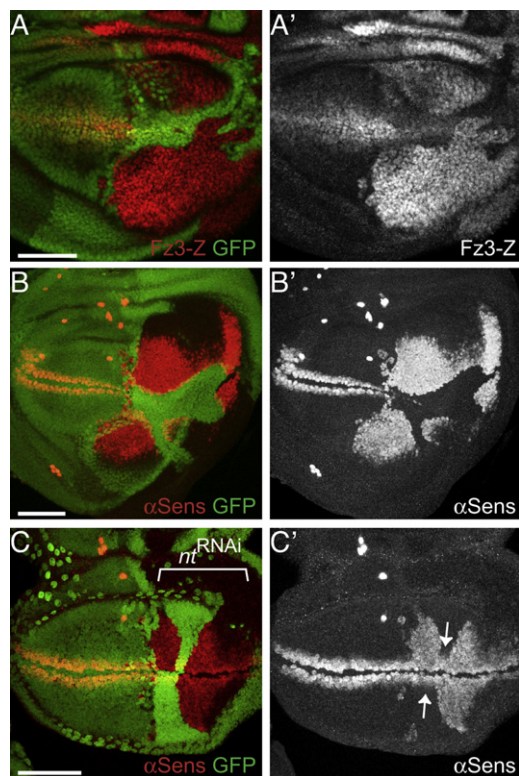


Figure 4. *axin* Mutant Cells Cause Notum-Dependent Downregulation of *sens* and *fz3* in Neighboring Wild-Type Cells

All panels in this figure show wing discs harboring *axin* mutant clones (GFP-negative) generated in the P compartment with *en-Gal4 UAS-FLP*, as in Figure 3D.

(A and A') Activity of a *fz3* reporter (*fz3-lacZ*) as detected with anti- β -galactosidase (red in [A] and white in [A']) is autonomously upregulated in *axin* mutant clones, as expected. Additionally, *fz3* expression in wild-type P cells is repressed by the presence of *axin* mutant patches.

(B and B') Wing disc harboring *axin* clones as above stained with anti-Sens (red in [B] and white in [B']). *sens* is ectopically expressed in *axin* cells as expected because of autonomous activation of Wg signaling. However, as with *fz3-lacZ*, expression of *sens* is abolished in wild-type P cells. This effect is fully penetrant (23 out of 23 discs).

(C and C') Discs of the same genotype as in (B), except that it also expresses a RNAi hairpin construct against *notum* in the P compartment (indicated by brackets). Staining with anti-Sens shows that expression in wild-type cells is restored (white arrows). This effect is also fully penetrant (19 out of 19 discs).

the effect on *dll* and *vg*, this suppression is fully penetrant (23 out of 23 discs) and appears unaffected by proximity to the A/P boundary. In summary, these results show that all Wg target genes tested are sensitive to nonautonomous negative feedback downstream of Wg signal transduction. However, they also suggest that *dll* and *vg* may be under additional regulatory control.

The Nonautonomous Inhibitory Activity of *axin* Mutant Cells Relies in Part on Notum

In order to identify relevant negative signals, we considered secreted molecules known to be expressed in response to Wg signaling. One good candidate was the secreted phospholipase

encoded by *notum*, also known as *wingful*. This gene is expressed in the cells flanking the source of Wg at the D/V boundary, and its product is a potent inhibitor of Wg signaling (Gerlitz and Basler, 2002; Giraldez et al., 2002; Kreuger et al., 2004). Notum and its mammalian homologs are thought to cleave off the GPI anchor of glypicans, known modulators of Wnt signaling (Kreuger et al., 2004; Traister et al., 2008). To test whether Notum accounts for the nonautonomous suppression of target gene expression by *axin* mutant cells, we generated *axin* mutant clones in P compartments expressing a hairpin construct against *notum*. Ectopic *sens* expression was still activated in the *axin* mutant cells as expected, but normal expression of *sens* was fully restored in wild-type cells (arrow in Figure 4C; 19 out of 19 discs). Therefore, *axin* mutant cells require Notum activity to suppress *sens* expression in surrounding cells. Importantly, however, Notum-deficient *axin* mutant patches (generated in the same genotype as above) still suppress *dll* expression in nearby wild-type cells (seen in six out of 15 discs; not shown). Therefore, Notum is not sufficient to account for the suppression of *dll* expression and is unlikely to mediate all of the nonautonomous inhibitory activity downstream of Wg signaling. As further evidence for an additional suppressing signal, we note here that the normalization of *dll* expression seen in large *axin* mutant patches (Figure 3D) still occurs in P compartments expressing the *notum* RNAi transgene (five out of ten discs).

Nonautonomous Inhibition from “Low/Medium Signaling” Cells

As illustrated in Figure 2, small patches of *fz fz2* mutant cells downregulate *dll* expression because, we suggest, while losing the positive input from signaling, they remain under an inhibitory influence spreading from surrounding Wg transducing cells. This inhibitory influence is unlikely to be mediated by Notum because Notum acts extracellularly and is therefore not expected to modulate signal transduction downstream of the receptors. Indeed, in Notum-deficient P compartments, *fz fz2* mutant patches still downregulate *dll* expression (Figure 5A). This observation confirms that another suppressive activity is at work and that it could be produced by cells that are not necessarily near the D/V boundary. To independently assess the ability of any pouch cells to suppress signal transduction in surrounding cells, we generated discs that are largely deficient in *fz fz2* with only one to two patches of wild-type (GFP-positive) tissue remaining. This is occasionally achieved with *ms209-Gal4* and *UAS-Flp* in a *Minute* background (see Figure 5B). As expected from the results described above (Figures S1C and S1C' and Figures 2E and 2E'), expression of *dll* is maintained in the mutant tissue despite the inability of cells to transduce the Wg signal. Strikingly, however, the *fz fz2* mutant cells that are surrounded by wild-type (GFP-positive; Wg-transducing) tissue downregulate *dll* expression (Figures 5B and 5B', arrows). We conclude that “normal” Wg signaling in the pouch triggers the production of a signal that depresses *dll* expression in surrounding cells. This signal is unlikely to involve Notch or EGFR signaling, as neither pathway on its own suppresses *vg* or *dll* expression in the pouch (Figure S6).

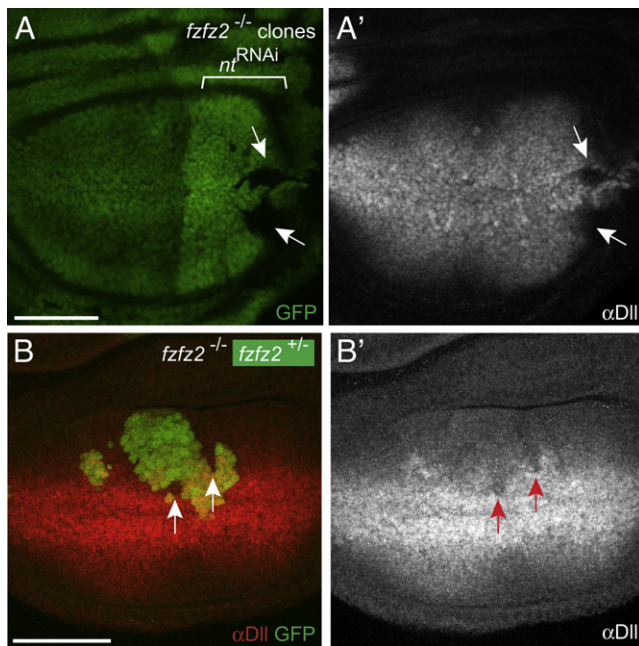


Figure 5. Notum-Independent Lateral Inhibition

(A and A') Wing disc carrying *fz fz2* clones generated with *en-Gal4 UAS-FLP* and at the same time expressing an RNAi hairpin construct against *notum* in the P compartment (indicated by brackets). The disc is stained with anti-Dll (white in [A']). Downregulation of *dll* expression (arrows) still occurs in the *fz fz2* mutant clones ([A], GFP-negative), suggesting that Notum is not required.

(B and B') Wing disc of genotype *UAS-FLP; fz fz2 FRT/M FRT; ms209-Gal4* stained as indicated. The disc is largely composed of *fz fz2* mutant (GFP-negative) cells. Only a few patches of wild-type (GFP-positive) cells remain. The majority of *fz fz2* mutant cells express normal levels of *dll*. However, *dll* expression is locally depressed in *fz fz2* mutant cells that are surrounded by wild-type cells (arrows).

Nonautonomous Negative Feedback Contributes to Precision of Cell Fate Specification

At least two nonautonomous inhibitory mechanisms are activated in Wg transducing cells. In the absence of these mechanisms, we expect that small groups of wild-type cells surrounded by signaling-deficient cells will become hypersensitive to Wg. Isolated wild-type cells located in the midst of *fz fz2* mutant territory were generated by inducing recombination with *sal-Gal4* and *UAS-Flp* in a *Minute* background. In agreement with our prediction, some of them express the bristle-inducing gene *sens* at ectopic locations (Figures 6A–6A', arrows; compare to wild-type in Figure 6B), an indication of excessive Wg signaling. To quantify this effect, we turned to adult wings, which can be obtained because this genetic background is not lethal. These wings lack bristles in parts of the margin area, as expected from the widespread elimination of Wg signal transduction. In addition, as shown in Figures 6C and 6C', ectopic bristles appear within the blade (2.5 ± 2 ectopic bristles per wing; $n = 35$). Ectopic bristles, which we define here as forming at a distance of five or more cell diameters away from the margin, are never seen in control, wild-type wings ($n > 100$). These results demonstrate that wild-type cells misread their position in the Wg

gradient if their neighbors cannot transduce the Wg signal and that downstream nonautonomous inhibition normally ensures that only the cells near the source of Wg activate the high-level target gene *sens*.

DISCUSSION

Here, we have explored how cells of *Drosophila* wing imaginal discs interpret the Wg gradient. As we report, removal of Wg signaling from the whole imaginal disc (or a whole compartment) leads to loss of *sens* expression, as expected, but has relatively little effect on the expression of *vg* and *dll*. Therefore, different target genes may be differentially regulated. Our experiments show that once the *vg* and *dll* expression domains are established in the pouch, they are expressed at self-sustained basal levels in the absence of Wg. Moreover, our observation that *vg* and *dll* continue to be expressed after abrogation of Wg signal transduction in large—but not small—patches of tissue suggests that Wg signaling exerts both a positive (direct) and a negative (indirect) influence on expression of these genes. We have identified two modes of Wg-dependent negative influence. One, as yet unidentified, arises from all the cells of the pouch that transduce the Wg signal and acts on *dll* and *vg* (and perhaps the other Wg targets). Another negative signal, encoded by *notum*, originates from the cells receiving a high dose of Wg and affects all Wg targets (Figures 7A and 7B).

Continued Expression of *dll* and *vg* Despite Wg Removal

Expression of *vg* and *dll* is activated throughout most of the pouch, the area of wing imaginal disc that gives rise to the wing proper. Numerous reports have shown that this activation is under the direct control of Wg and operates continuously throughout imaginal disc development. Indeed, preventing Wg signal transduction in small patches of tissue invariably leads to the downregulation of target genes, including *dll* and *vg* (Belenkaya et al., 2002; Chen and Struhl, 1999; Hoffmans et al., 2005; Neumann and Cohen, 1997; Wehrli et al., 2000; Zecca et al., 1996). This is true even if signal transduction is eliminated during the third larval instar. Considering this body of evidence, it is surprising that expression of these target genes is maintained after complete removal of Wg signaling during imaginal disc development. We conclude that proximodistal patterning of the wing does not rely continuously on the Wg gradient. One possibility is that expression of *dll* and *vg*, which requires Wg signaling for its establishment early in disc development, can later self-maintain in the absence of continuous input from Wg. Accordingly, at these later stages, Wg signaling would act to refine and fashion a pre-existing pattern of expression (see also Martinez Arias, 2003). Thus, throughout normal development, the expression of *dll* and *vg* would be subject to Wg-dependent negative and positive regulation. In addition, “free-running” expression of *dll* and *vg* may be subject to negative regulation originating from the tissue surrounding the prospective wing region (E.P. and J.-P.V., unpublished data), thus possibly explaining why a gradient is maintained even in the absence of Wg. The behavior of *dll* and *vg* suggests that our understanding of how the Wg gradient specifies cell fates must be revised. It also implies that an inhibitory signal is produced by cells undergoing Wg signal transduction.

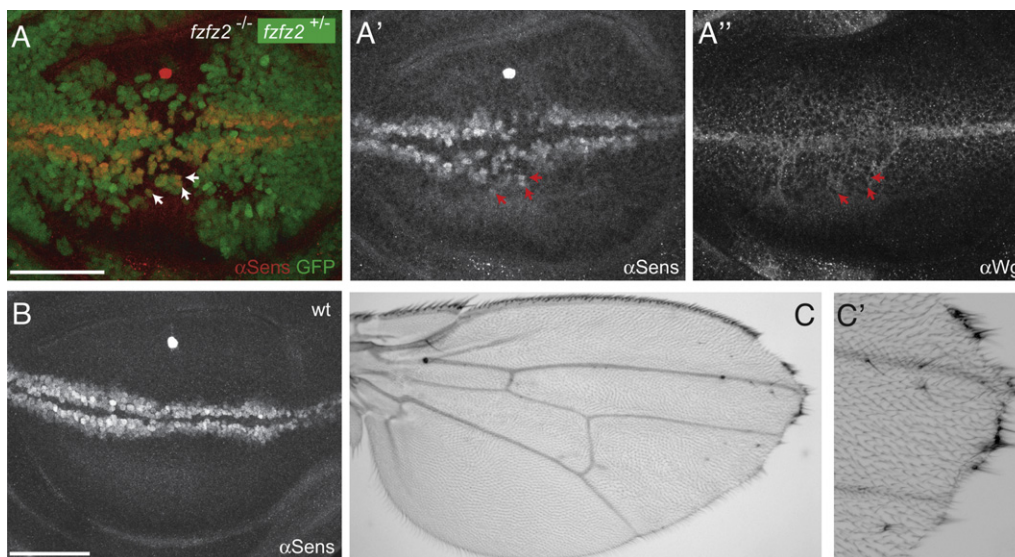


Figure 6. Nonautonomous Negative Feedback Contributes to Precision of Cell Fate Specification

(A–A'') Wing disc of genotype *sal-Gal4 UAS-FLP; fz fz2 FRT/M FRT* stained as indicated. In this genotype, a few isolated wild-type cells (GFP positive) find themselves in a central patch of *fz fz2* mutant cells. Some of these wild-type cells ectopically activate *sens* expression ([A] and [A'], arrows).

(B) Expression of *sens* in a wild-type disc.

(C and C') Adult wing of the same genotype as in (A). Margin tissue is lost as expected from the loss of *fz fz2*. (C') Higher magnification of the distal region showing the presence of ectopic bristles inside the blade area (2.5 ± 2 ectopic bristles; $n = 35$). Therefore, in this genotype, mutant cells fail to make margin bristles, while residual wild-type cells make bristles too readily.

Two Distinct Inhibitory Signals Downstream of Wg Signaling

Our data suggest that two distinct mechanisms contribute to the nonautonomous inhibitory activity downstream of Wg signaling. One negative signal is activated near the Wg source in response to strong activation of the Wg signal transduction pathway, while another is produced by all the cells of the pouch, again in response to Wg signaling (Figure 7A). Although we presume that all target genes are affected by both mechanisms, we have not shown directly that the unknown signal modulates expression of *sens* and *fz3* (Figure 7B).

Upon high activation of Wg signaling, cells produce a signal that inhibits Wg signal transduction in surrounding cells. This is best illustrated by the behavior of *axin* mutant cells, which activate signal transduction maximally. Large patches of *axin* mutant cells suppress the expression of all target genes in surrounding cells. Although the nonautonomous suppression of *sens* and *fz3* by *axin* mutant cells is fully penetrant, that of *vg* and *dll* is more variable, perhaps reflecting the fact that expression of these genes is controlled by additional regulators beside Wg. Through candidate testing, we identified Notum, which is expressed in response to high Wg signaling, as one signal involved in this nonautonomous inhibition. Indeed, RNAi-mediated Notum knockdown prevents *axin* mutant cells from suppressing *sens* expression in nearby cells.

Notum is unlikely to account for all of the nonautonomous inhibitory activity originating from high signaling cells, since *dll* expression is still suppressed by Notum-deficient, *axin* mutant cells (data not shown). This suggests that an additional negative signal is produced in response to high level Wg signal transduction and that *dll* and *vg* are more sensitive to this inhibitory

activity than *sens* and *fz3*. This signal could be the same as that produced by cells undergoing intermediate/low Wg signaling (Figure 5B), as the latter signal too acts on *dll* and *vg* and is not mediated by *notum*. We suggest that this widespread negative signal could account for the downregulation of *dll* and *vg* expression in small *fz fz2* mutant patches. We propose that, in addition to providing a positive input on *dll/vg* gene expression, Wg signaling causes every pouch cell to produce a secondary signal that downregulates these genes, acting below the level of the Fz receptor complex. Thus, in wild-type tissue, every cell integrates the positive and negative signals and modulates pre-existing expression of *dll* and *vg* accordingly. In the complete absence of Wg signaling, neither the positive nor the negative signal is produced, and expression of these genes remains relatively unaffected. However, when cells that cannot transduce the Wg signal (e.g., *fz fz2* mutant) are surrounded by wild-type cells (Figure 7C), the mutant cells are no longer receiving the positive input while they remain sensitive to the negative signal generated around them, and, as a result, they downregulate *dll* and *vg* expression. This signal is probably not juxtacrine (as it reaches inside *fz fz2* patches) and indeed is not mediated by Notch. EGFR also appears not to be involved. So far the signal remains unidentified; it could be mediated by a secreted protein or by a less defined influence such as, for example, mechanical tension.

Benefits of Nonautonomous Inhibition

Competing influence from activators and inhibitors is a common regulatory theme in development. As illustrated in the case of the zebrafish mesoderm, Squint (the activator) and Lefty (the

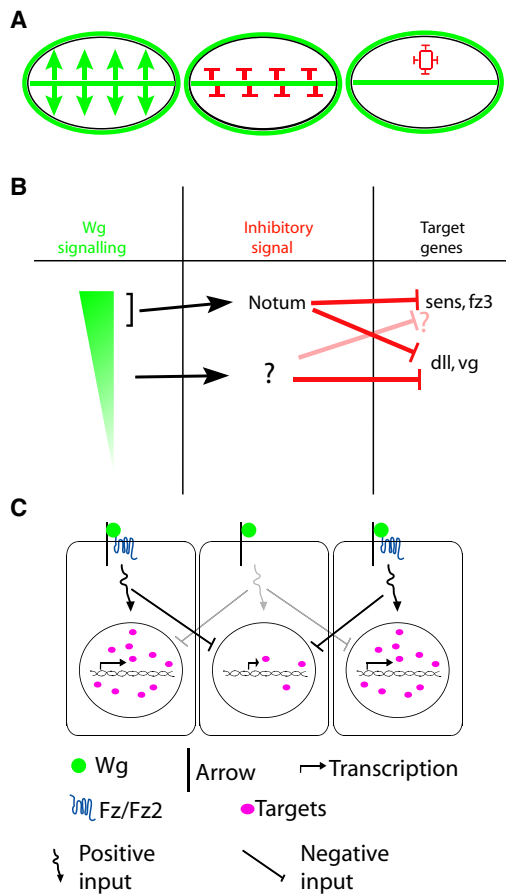


Figure 7. Nonautonomous Negative Feedback Shapes Proximodistal Patterning

(A) Proximodistal patterning of the wing relies on three influences triggered by Wg signaling. Wg produced at the D/V boundary forms a concentration gradient that activates target genes (left). In response to high level Wg, cells produce Notum, an extracellular inhibitor of Wg signaling (center). In addition, Wg signal transduction triggers pouch cells to produce another signal that represses target genes in their vicinity (right; see also [C]).

(B) Summary of the negative regulatory activities triggered by Wg signaling. Interactions based on evidence are depicted by solid bars, whereas the shaded bar shows a potential but unconfirmed interaction. Cells exposed to high Wg levels produce Notum, which suppresses the expression of all Wg target genes tested (see also Gerlitz and Basler, 2002; Giraldez et al., 2002). In addition, all pouch cells responding to Wg produce an inhibitor, of as yet unidentified nature, that inhibits *dll* and *vg* (and potentially *sens* and *fz3*) in neighboring cells.

(C) Lateral inhibition shapes the response of *dll* and *vg* to Wg signaling. Expression of Wg target genes is regulated by a combination of negative and positive inputs. Activation of Wg signal transduction within each cell provides the positive input (in a dose-dependent manner). This also leads to the production of a signal that negatively regulates target gene expression in surrounding cells. In the complete absence of Wg signal transduction (e.g., *fz fz2* mutant discs), cells receive neither the positive nor the negative input, and target genes are relatively unaffected. A different result is seen when non-signaling cells are confronted with normal cells (e.g., when the tissue is a mosaic of *fz fz2* mutant and wild-type clones, as exemplified in this panel). The central, non-signaling cell can no longer receive the positive input from Wg signal transduction while still remaining sensitive to the negative signal from nearby cells. As a result, pre-existing expression of *dll* and *vg* is downregulated.

long-range inhibitor) form a classical reaction-diffusion system (Meinhardt, 2001; Chen and Schier, 2002; Feldman et al., 2002; Schier, 2003). In such systems, the inhibitor's primary function is to limit the range of action of the activator far from the source while the activator dominates near the source. By contrast, Notum suppresses gene expression in nearby surrounding tissue, suggesting short-range lateral inhibition, perhaps in addition to longer range of action. Moreover, Notum and Wg do not fulfill all the criteria of a reaction-diffusion system since Notum has no impact on Wg expression. In our view, the key regulatory feature of proximodistal patterning in the wing is the fact that Wg originating from the D/V boundary triggers a form of nonautonomous negative feedback akin to lateral inhibition. This feedback is mediated by two inhibitory signals, one originating near the Wg source and the other from all responding cells.

In sensory processing, lateral inhibition is an essential component of contrast enhancement and dark adaptation (Masland, 2005). We suggest that the interpretation of morphogen gradients would equally benefit from such features. Thus, nonautonomous negative feedback is expected to sharpen the cells' response within the gradient. Near the source of Wg, nonautonomous feedback inhibitors (probably dominated by Notum) may ensure the formation of a sharp boundary of *sens* expression. This suggestion is supported by our finding that *sens* becomes ectopically expressed (causing ectopic sensory bristles to form) when nonautonomous inhibition is eliminated by preventing surrounding cells from responding to Wg. Further away from the boundary, our data suggest that all the cells of the pouch mutually inhibit each other's response to Wg. As a result, the interpretation of the Wg gradient is continuously adjusted (normalized) much like the retina adjusts to different light levels during dark adaptation (Masland, 2005). A graphic illustration of this property comes from our observation that *axin* cells frequently fail to upregulate *Dll* when they constitute the majority of a compartment. Note here that this process affects *dll* and *vg*, not *sens*, and occurs even when Notum is knocked down. Since normalization affects *dll* expression autonomously activated by the loss of *axin*, it must involve a signal that impinges downstream of *axin*, possibly even on another signaling pathway that regulates *dll* and *vg*. Normalization may render pattern formation more resistant to variations in morphogen production and may explain why many morphogens are insensitive to gene dosage. It may also explain why cells appear to respond to the slope of morphogen gradients rather than to the absolute level (Day and Lawrence, 2000; Rogulja and Irvine, 2005).

Conclusion

One important implication of our findings is that, in vivo, cells do not simply read the absolute level of Wg that they are exposed to (as stipulated by the French flag model; Wolpert [1969]). Clearly, the local level of Wg is important, but the ultimate response is shaped by secondary cell interactions. Cells integrate information from their neighbors to read the Wg gradient. We suggest that secondary interactions are needed for cells to process the information contained in the original gradient and achieve patterning precision.

EXPERIMENTAL PROCEDURES

Fly Stocks

The following fly stocks were used: *FRT40A* (Bloomington), *hh-Gal4* (J. Casal), *yw Ubx-FLP* (F. Schweisguth), *wg^{cx4} FRT40A/Gla Bc* (I. Salecker), *yw hs-FLP*; *M(2)24F¹ arm-lacZ FRT40A/CyO* (I. Guerrero), *yw hs-FLP*; *Sp/Gla Bc*; *Dfz1^{P21}Dfz2^{C2} ri FRT2A/TM6* (G. Struhl), *yw*; *M(3)⁵⁵ p[nls-GFP]FRT2A/TM6* (F. Schweisguth), *yw hs-FLP*; *ubi-GFP FRT2A* (A. Gould), *M(2)24F¹ FRT40A/CyO* (Bloomington), *en-Gal4 UAS-FLP* (J. Casal), *FRT82 axin^h / TM6* (M. Bienz), *FRT82B ubi-GFP* (Bloomington), *w*; *FRT82B ubi-GFP Rps3/TM6* (Bloomington), *sal-Gal4/CyO* (L.A. Baena Lopez), *ci-Gal4/CyO* (L.A. Baena Lopez), *UAS-FLP* (Bloomington), *ms209-Gal4/ ci^D* (I. Guerrero), *UAS-wg^{RNAi} UAS-Dcr/TM6* (VDRC and B. Dickson, respectively, recombined for this study), *cycE ubi-GFP FRT40A/ Gla Bc* (I. Salecker), *wg^{ts} FRT40A/ Gla Bc* (recombined for this study), *FRT82B apc²⁹¹⁰ apc^{Q8}/TM6* (M. Peifer), *UAS-nt^{RNAi}* (VDRC), *UAS-N^{inttra}* (S. Bray), *UAS-CD8-GFP hsFLP*; *tub-Gal80 FRT40*; *tub-Gal4/ TM6* (S. Cohen), *tkv^{str11} FRT40A/ CyO-GFP* (M. Gonzalez-Gaitan), *FRT42D flb^{K35} / CyO* (M. Freeman), *UAS-CD8-GFP hsFLP*; *FRT42D tub-Gal80*; *tub-Gal4/TM6* (S. Cohen), and *fz3²⁹* (T. Kojima).

Experimental Genotypes

Genotypes are listed below by figure panel.

Figures 1A, 1C, and 1E: Wild-type

Figures 1B, 1D, 1F, and 1I: *Ubx-FLP/+*; *wg^{cx4} FRT40A/ M(2)24F¹ arm-lacZ FRT40A*

Figure 1G: *Ubx-FLP/+*; *FRT40A/ M(2)24F¹ arm-lacZ FRT40A*

Figure 1K: *Ubx-FLP/+*; *Dfz1^{P21}Dfz2^{C2} ri FRT2A/ ubi-GFP FRT2A*

Figures 2A–2D: *wg^{cx4} FRT40A/ M(2)24F¹ FRT40A*; *hh-Gal4 UAS-FLP/+*

Figure 2E: *en-Gal4 UAS-FLP/+*; *Dfz1^{P21}Dfz2^{C2} ri FRT2A/ M(3)⁵⁵ p[nls-GFP]FRT2A*

Figure 2F: *en-Gal4 UAS-FLP/+*; *Dfz1^{P21}Dfz2^{C2} ri FRT2A/ ubi-GFP FRT2A*

Figure 3A: *yw hs-FLP/+*; *FRT82B axin^h / FRT82B ubi-GFP*

Figure 3C: *yw hs-FLP/+*; *FRT82B axin^h / FRT82B ubi-GFP Rps3*

Figure 3D: *en-Gal4 UAS-FLP/+*; *FRT82B axin^h / FRT82B ubi-GFP*

Figure 4A: *fz3²⁹ /+*; *en-Gal4 UAS-FLP/+*; *FRT82B axin^h / FRT82B ubi-GFP*

Figures 4B and 4C: *en-Gal4 UAS-FLP/+*; *FRT82B axin^h / FRT82B ubi-GFP*

Figure 5A: *en-Gal4 UAS-FLP/ UAS-nt^{RNAi}*; *Dfz1^{P21}Dfz2^{C2} ri FRT2A/ ubi-GFP FRT2A*

Figure 5B: *UAS-FLP/+*; *Dfz1^{P21}Dfz2^{C2} ri FRT2A/ M(3)⁵⁵ p[nls-GFP]FRT2A*; *ms209-Gal4/+*

Figures 6A and 6C: *sal-Gal4/ UAS-FLP*; *Dfz1^{P21}Dfz2^{C2} ri FRT2A/ M(3)⁵⁵ p[nls-GFP]FRT2A*

Figure 6B: Wild-type

Antibody Staining

The following primary antibodies were used: mouse anti-Wg 4D4 (prepared from cells obtained from the DSHB), guinea pig anti-Sens (a gift of H. Bellen), rabbit anti-Vg (gift of S. Carroll), mouse anti-Dll (gift of I. and D. Duncan), and rabbit anti- β -galactosidase (Cappel, Durham). Secondary antibodies used were Alexa-conjugated anti-mouse, anti-rabbit (Molecular Probes, Eugene), and Cy3-conjugated anti-guinea pig (Jackson ImmunoResearch, Pennsylvania). Unless otherwise indicated, a standard antibody staining technique was used for wing imaginal disc labeling. Double staining of anti-Wg and anti-Dll (both raised in mouse) was performed by staining first with anti-Dll and anti-mouse according to standard protocols and then performing a second staining with anti-Wg that had been fluorescently prelabelled with the Zenon antibody labeling kit (Invitrogen, Inc).

Heat Shock Induction of Mutant Clones

Mutant clones were generated by heat shocking of larvae for 1 hr at 37°C at 72 hr (\pm 12 hr) after egg laying. Larvae were dissected about 2 days after clone induction.

Wing Mounting and Bristle Quantification

Wings were mounted in Euparal (Agar Scientific). Ectopic bristle quantification in *sal-Gal4/ UAS-FLP*; *Dfz1^{P21}Dfz2^{C2} ri FRT2A/ M(3)⁵⁵ p[nls-GFP]FRT2A*

wings was done by scoring of bristles that were at least five cell diameters away from the wing margin.

Imaging and Image Analysis

Images were acquired with a Leica SP5 confocal microscope. Except for Figures 1A–1D and Figures 4A and 4B (green channel only), which show a single confocal slice, micrographs are projections (maximum intensity) of a stack of at least ten sections taken at 1 μ m intervals. All fluorescent intensity quantifications were performed with the software package ImageJ (<http://rsb.info.nih.gov/ij/>). Where comparison between separate discs was required, fluorescence intensity was measured in regions of interest (ROIs) of identical sizes and shapes and drawn at equivalent locations within each disc. For *Ubx-FLP*-induced *wg* mutant discs, a separate batch of control discs was dissected, stained, and imaged in parallel with identical settings. For discs containing *Ubx-FLP*-induced *fz fz2* mutant clones, both control and mutant discs were obtained from the same cross. Thus, discs from a single batch could be prepared and imaged under identical conditions.

SUPPLEMENTAL DATA

Supplemental Data include Supplemental Experimental Procedures and six figures and can be found with this article online at [http://www.cell.com/supplemental/S0092-8674\(08\)01511-0](http://www.cell.com/supplemental/S0092-8674(08)01511-0).

ACKNOWLEDGMENTS

This work was supported by the Medical Research Council of Great Britain and the Endotrack (Framework 6) program of the European Union. We thank Hugo Bellen, Ian and Dianne Duncan, Sean Carrol, and the Developmental Studies Hybridoma Bank (Iowa University) for antibodies. We also thank the Bloomington Stock Center (Indiana University) and scientists listed in the [Experimental Procedures](#) for numerous *Drosophila* strains. We thank Cyrille Alexandre, Seth Blair, Sarah Bray, James Briscoe, Rafael Carazo-Salas, Jose Casal, Alex Gould, Nick Monk, Iris Salecker, and Francois Schweisguth for discussions and/or comments to the manuscript.

Received: February 5, 2008

Revised: September 24, 2008

Accepted: November 21, 2008

Published: January 22, 2009

REFERENCES

- Akong, K., Grevengoed, E.E., Price, M.H., McCartney, B.M., Hayden, M.A., DeNofrio, J.C., and Peifer, M. (2002). *Drosophila* APC2 and APC1 play overlapping roles in wingless signaling in the embryo and imaginal discs. *Dev. Biol.* 250, 91–100.
- Ashe, H.L., and Briscoe, J. (2006). The interpretation of morphogen gradients. *Development* 133, 385–394.
- Belenkaya, T.Y., Han, C., Standley, H.J., Lin, X., Houston, D.W., Heasman, J., and Lin, X. (2002). *pygopus* Encodes a nuclear protein essential for wingless/Wnt signaling. *Development* 129, 4089–4101.
- Chen, C.M., and Struhl, G. (1999). Wingless transduction by the Frizzled and Frizzled2 proteins of *Drosophila*. *Development* 126, 5441–5452.
- Chen, Y., and Schier, A.F. (2002). Lefty proteins are long-range inhibitors of squint-mediated nodal signaling. *Curr. Biol.* 12, 2124–2128.
- Day, S.J., and Lawrence, P.A. (2000). Measuring dimensions: the regulation of size and shape. *Development* 127, 2977–2987.
- Dessaud, E., Yang, L.L., Hill, K., Cox, B., Ulloa, F., Ribeiro, A., Mynett, A., Novitsch, B.G., and Briscoe, J. (2007). Interpretation of the sonic hedgehog morphogen gradient by a temporal adaptation mechanism. *Nature* 450, 717–720.

- Eldar, A., Rosin, D., Shilo, B.Z., and Barkai, N. (2003). Self-enhanced ligand degradation underlies robustness of morphogen gradients. *Dev. Cell* 5, 635–646.
- Eldar, A., Shilo, B.Z., and Barkai, N. (2004). Elucidating mechanisms underlying robustness of morphogen gradients. *Curr. Opin. Genet. Dev.* 14, 435–439.
- Feldman, B., Concha, M.L., Saude, L., Parsons, M.J., Adams, R.J., Wilson, S.W., and Stemple, D.L. (2002). Lefty antagonism of Squint is essential for normal gastrulation. *Curr. Biol.* 12, 2129–2135.
- Fuccillo, M., Joyner, A.L., and Fishell, G. (2006). Morphogen to mitogen: the multiple roles of hedgehog signalling in vertebrate neural development. *Nat. Rev. Neurosci.* 7, 772–783.
- Gerlitz, O., and Basler, K. (2002). Wingful, an extracellular feedback inhibitor of Wingless. *Genes Dev.* 16, 1055–1059.
- Giraldez, A.J., Copley, R.R., and Cohen, S.M. (2002). HSPG modification by the secreted enzyme Notum shapes the Wingless morphogen gradient. *Dev. Cell* 2, 667–676.
- Gregor, T., Tank, D.W., Wieschaus, E.F., and Bialek, W. (2007). Probing the limits to positional information. *Cell* 130, 153–164.
- Gurdon, J.B., and Bourillot, P.Y. (2001). Morphogen gradient interpretation. *Nature* 413, 797–803.
- Gurdon, J.B., Dyson, S., and St Johnston, D. (1998). Cells' perception of position in a concentration gradient. *Cell* 95, 159–162.
- Gurdon, J.B., Standley, H., Dyson, S., Butler, K., Langon, T., Ryan, K., Stenard, F., Shimizu, K., and Zorn, A. (1999). Single cells can sense their position in a morphogen gradient. *Development* 126, 5309–5317.
- Hamada, F., Tomoyasu, Y., Takatsu, Y., Nakamura, M., Nagai, S., Suzuki, A., Fujita, F., Shibuya, H., Toyoshima, K., Ueno, N., et al. (1999). Negative regulation of Wingless signaling by D-axin, a Drosophila homolog of axin. *Science* 283, 1739–1742.
- Hart, M.J., de los Santos, R., Albert, I.N., Rubinfeld, B., and Polakis, P. (1998). Downregulation of beta-catenin by human Axin and its association with the APC tumor suppressor, beta-catenin and GSK3 beta. *Curr. Biol.* 8, 573–581.
- Hoffmans, R., Stadel, R., and Basler, K. (2005). Pygopus and legless provide essential transcriptional coactivator functions to armadillo/beta-catenin. *Curr. Biol.* 15, 1207–1211.
- Howard, M., and ten Wolde, P.R. (2005). Finding the center reliably: robust patterns of developmental gene expression. *Phys. Rev. Lett.* 95, 208103.
- Ikeda, S., Kishida, S., Yamamoto, H., Murai, H., Koyama, S., and Kikuchi, A. (1998). Axin, a negative regulator of the Wnt signaling pathway, forms a complex with GSK-3beta and beta-catenin and promotes GSK-3beta-dependent phosphorylation of beta-catenin. *EMBO J.* 17, 1371–1384.
- Jaeger, J., Irons, D., and Monk, N. (2008). Regulative feedback in pattern formation: towards a general relativistic theory of positional information. *Development* 135, 3175–3183.
- Jaiswal, M., Agrawal, N., and Sinha, P. (2006). Fat and Wingless signaling oppositely regulate epithelial cell-cell adhesion and distal wing development in Drosophila. *Development* 133, 925–935.
- Kerszberg, M., and Wolpert, L. (2007). Specifying positional information in the embryo: looking beyond morphogens. *Cell* 130, 205–209.
- Kiecker, C., and Niehrs, C. (2001). A morphogen gradient of Wnt/beta-catenin signalling regulates anteroposterior neural patterning in Xenopus. *Development* 128, 4189–4201.
- Klein, T., and Arias, A.M. (1999). The vestigial gene product provides a molecular context for the interpretation of signals during the development of the wing in Drosophila. *Development* 126, 913–925.
- Kreuger, J., Perez, L., Giraldez, A.J., and Cohen, S.M. (2004). Opposing activities of Dally-like glypican at high and low levels of Wingless morphogen activity. *Dev. Cell* 7, 503–512.
- Lawrence, P.A. (2001). Morphogens: how big is the big picture? *Nat. Cell Biol.* 3, E151–E154.
- Liem, K.F., Jr., Jessell, T.M., and Briscoe, J. (2000). Regulation of the neural patterning activity of sonic hedgehog by secreted BMP inhibitors expressed by notochord and somites. *Development* 127, 4855–4866.
- Martinez Arias, A. (2003). Wnts as morphogens? The view from the wing of Drosophila. *Nat. Rev. Mol. Cell Biol.* 4, 321–325.
- Masland, R.H. (2005). Sensory systems: fine-tuning the visual scene. *Curr. Biol.* 15, R808–R810.
- McHale, P., Rappel, W.J., and Levine, H. (2006). Embryonic pattern scaling achieved by oppositely directed morphogen gradients. *Phys. Biol.* 3, 107–120.
- Meinhardt, H. (2001). Organizer and axes formation as a self-organizing process. *Int. J. Dev. Biol.* 45, 177–188.
- Morata, G., and Lawrence, P.A. (1977). The development of wingless, a homeotic mutation of Drosophila. *Dev. Biol.* 56, 227–240.
- Morata, G., and Ripoll, P. (1975). Minutes: mutants of drosophila autonomously affecting cell division rate. *Dev. Biol.* 42, 211–221.
- Neumann, C.J., and Cohen, S.M. (1997). Long-range action of Wingless organizes the dorsal-ventral axis of the Drosophila wing. *Development* 124, 871–880.
- Ng, M., Diaz-Benjumea, F.J., Vincent, J.P., Wu, J., and Cohen, S.M. (1996). Specification of the wing by localized expression of wingless protein. *Nature* 381, 316–318.
- Nolo, R., Abbott, L.A., and Bellen, H.J. (2000). Senseless, a Zn finger transcription factor, is necessary and sufficient for sensory organ development in Drosophila. *Cell* 102, 349–362.
- Nordstrom, U., Jessell, T.M., and Edlund, T. (2002). Progressive induction of caudal neural character by graded Wnt signaling. *Nat. Neurosci.* 5, 525–532.
- Patten, I., and Placzek, M. (2002). Opponent activities of Shh and BMP signaling during floor plate induction in vivo. *Curr. Biol.* 12, 47–52.
- Phillips, R.G., and Whittle, J.R. (1993). wingless expression mediates determination of peripheral nervous system elements in late stages of Drosophila wing disc development. *Development* 118, 427–438.
- Rogulja, D., and Irvine, K.D. (2005). Regulation of cell proliferation by a morphogen gradient. *Cell* 123, 449–461.
- Sato, A., Kojima, T., Ui-Tei, K., Miyata, Y., and Saigo, K. (1999). Dfrizzled-3, a new Drosophila Wnt receptor, acting as an attenuator of Wingless signaling in wingless hypomorphic mutants. *Development* 126, 4421–4430.
- Schier, A.F. (2003). Nodal signaling in vertebrate development. *Annu. Rev. Cell Dev. Biol.* 19, 589–621.
- Sharma, R.P., and Chopra, V.L. (1976). Effect of the Wingless (wg1) mutation on wing and haltere development in Drosophila melanogaster. *Dev. Biol.* 48, 461–465.
- Sivasankaran, R., Calleja, M., Morata, G., and Basler, K. (2000). The Wingless target gene Dfz3 encodes a new member of the Drosophila Frizzled family. *Mech. Dev.* 91, 427–431.
- Strigini, M., and Cohen, S.M. (1999). Formation of morphogen gradients in the Drosophila wing. *Semin. Cell Dev. Biol.* 10, 335–344.
- Traister, A., Shi, W., and Filmus, J. (2008). Mammalian Notum induces the release of glypicans and other GPI-anchored proteins from the cell surface. *Biochem. J.* 410, 503–511.
- Turing, A.M. (1952). The chemical basis of morphogenesis. *Philosophical Transactions of the Royal Society of London B* 237, 37–72.
- Vincent, J.P., and Briscoe, J. (2001). Morphogens. *Curr. Biol.* 11, R851–R854.
- Wang, S.H., Simcox, A., and Campbell, G. (2000). Dual role for Drosophila epidermal growth factor receptor signaling in early wing disc development. *Genes Dev.* 14, 2271–2276.
- Wehrli, M., Dougan, S.T., Caldwell, K., O'Keefe, L., Schwartz, S., Vaizel-Ohayon, D., Schejter, E., Tomlinson, A., and DiNardo, S. (2000). arrow encodes an LDL-receptor-related protein essential for Wingless signalling. *Nature* 407, 527–530.
- Wolpert, L. (1969). Positional information and the spatial pattern of cellular differentiation. *J. Theor. Biol.* 25, 1–47.

Wu, J., and Cohen, S.M. (2002). Repression of Teashirt marks the initiation of wing development. *Development* 129, 2411–2418.

Xu, T., and Rubin, G.M. (1993). Analysis of genetic mosaics in developing and adult *Drosophila* tissues. *Development* 117, 1223–1237.

Zecca, M., and Struhl, G. (2007). Recruitment of cells into the *Drosophila* wing primordium by a feed-forward circuit of vestigial autoregulation. *Development* 134, 3001–3010.

Zecca, M., Basler, K., and Struhl, G. (1996). Direct and long-range action of a wingless morphogen gradient. *Cell* 87, 833–844.

Zeng, L., Fagotto, F., Zhang, T., Hsu, W., Vasicek, T.J., Perry, W.L., 3rd, Lee, J.J., Tilghman, S.M., Gumbiner, B.M., and Costantini, F. (1997). The mouse Fused locus encodes Axin, an inhibitor of the Wnt signaling pathway that regulates embryonic axis formation. *Cell* 90, 181–192.